

# Silver- and Silver–Hydrogen-Related Defects in Silicon


Katarzyna Gwozdz and Vladimir Kolkovsky\*

Herein, the electrical and structural properties of Ag- and AgH-related defects in n- and p-type Si are reinvestigated using conventional deep-level transient spectroscopy (DLTS) and high-resolution Laplace DLTS. It is evidenced that a peak corresponding to substitutional Ag does not always appear in as-grown Si and additional heat treatments are necessary to observe this defect. Several AgH-related peaks, which were not previously reported in the literature, are observed in hydrogenated n- and p-type Si. The electrical properties of these defects are determined and their origin is discussed. By using high-resolution Laplace DLTS, the depth profiles of AgH-related defects previously assigned to  $\text{Ag}_5\text{H}$  and  $\text{Ag}_5\text{H}_2$  are analyzed, and their assignments are questioned.

## 1. Introduction

The study of the electrical properties of transition metals (TM) in Si and their interaction with hydrogen still attracts significant interest since these impurities could significantly decrease the lifetime of minority carriers. In modern microelectronics silicon wafers can be often contaminated with TM in various technological steps. The electrical and optical properties of silver-related defects in crystalline Si have been extensively studied in the literature.<sup>[1–14]</sup> Similar to gold substitutional silver should also introduce two deep levels in the band gap of Si: the single acceptor state at around 0.5–0.59 eV below the conduction band<sup>[2,3,7,8,10,12]</sup> and the single donor state at about 0.34–0.41 eV above the valence band.<sup>[2,3,7,8,10,12]</sup> Until now the origin of the scatter of the activation energy of  $\text{Ag}_5$  observed in different studies is not understood. In addition, some shallower Ag-related levels were also reported using Hall effect measurements or by the metal oxide semiconductor technique.<sup>[1,4,5]</sup>

K. Gwozdz  
 Department of Quantum Technologies  
 University of Science and Technology  
 Wrocław University of Science and Technology  
 Wybrzeże Wyspiańskiego 27, 50-370 Wrocław, Poland  
 V. Kolkovsky  
 Department EMT  
 Fraunhofer IPMS  
 Dresden Maria-Reiche Str. 2, 01109 Dresden, Germany  
 E-mail: uladzimir.kalkouski@ipms.fraunhofer.de

 The ORCID identification number(s) for the author(s) of this article can be found under <https://doi.org/10.1002/pssa.202100217>.

© 2021 The Authors. physica status solidi (a) applications and materials science published by Wiley-VCH GmbH. This is an open access article under the terms of the Creative Commons Attribution License, which permits use, distribution and reproduction in any medium, provided the original work is properly cited.

DOI: 10.1002/pssa.202100217

In hydrogenated samples, H interacts with Ag forming various AgH-related complexes (E2, E3, E5, H2, E6, and H3). Their electrical properties were investigated in n- and p-type Si in Yarykin et al.<sup>[12]</sup> By analyzing depth profiles of the defects E3, E2, and H2 were attributed to different charge states of AgH, whereas E6 and H3 were assigned to different charge states of  $\text{AgH}_2$ . One should note that E6 has never been explicitly observed by deep-level transient spectroscopy (DLTS), and its existence was deduced from the comparison of the depth profiles of E2 and E3, which were not identical at depths close to the surface of n-type Si. Yarykin et al.<sup>[12]</sup> proposed that E6 could have similar electrical properties to those of E2 and, therefore, these defects could not be properly resolved by the conventional DLTS technique.<sup>[12]</sup> This hypothesis was used as an explanation for the different depth profiles of E2 and E3.

In the present study, we reinvestigate the electrical properties of Ag and AgH-related defects in as-grown samples after wet chemical etching and subsequent annealing at 500 °C by using the high-resolution Laplace DLTS technique.<sup>[15]</sup>

## 2. Results

Figure 1 shows DLTS spectra recorded in three different samples (#1, #2, and #3) after WCE and after annealing at 500 °C. All spectra were recorded close to the surface with a reverse bias of −4 V and a filling pulse of 0 V. Four peaks, labelled  $\text{E35}_{\text{AgH}}$ ,  $\text{E44}_{\text{AgH}}$ , CH, and  $\text{E100}_{\text{AgH}}$ , were observed in sample #1 after WCE. By comparing the electrical properties of the peaks with those known from the literature<sup>[16]</sup> we assign CH to the single acceptor state of the carbon-hydrogen complex.  $\text{E35}_{\text{AgH}}$ ,  $\text{E44}_{\text{AgH}}$ , and  $\text{E100}_{\text{AgH}}$  have not been previously reported in the literature. In addition to these levels we did not observe any other DLTS peaks deeper in the bulk of Si by measuring with a reverse bias of −8 V and a filling pulse of −4 V. The Ag related peaks  $\text{E35}_{\text{AgH}}$ ,  $\text{E44}_{\text{AgH}}$ , and  $\text{E100}_{\text{AgH}}$  disappear after the annealing at 500 °C and another defect labelled  $\text{Ag}(-/0)$  becomes dominant in the DLTS spectrum. Similar DLTS peaks as  $\text{Ag}(-/0)$  have been already reported in the previous studies.<sup>[2,3,7,8,10,12]</sup> and we attribute this level to the single acceptor state of substitutional Ag. In addition to this dominant defect, several small DLTS peaks  $\text{E108}_{\text{Ag}}$  and  $\text{E148}_{\text{Ag}}$  can be distinguished at lower temperatures in the annealed sample. These defects were observed close to the surface as well as deeper in the bulk. The electrical and annealing properties of  $\text{E148}_{\text{Ag}}$  are very similar to that of

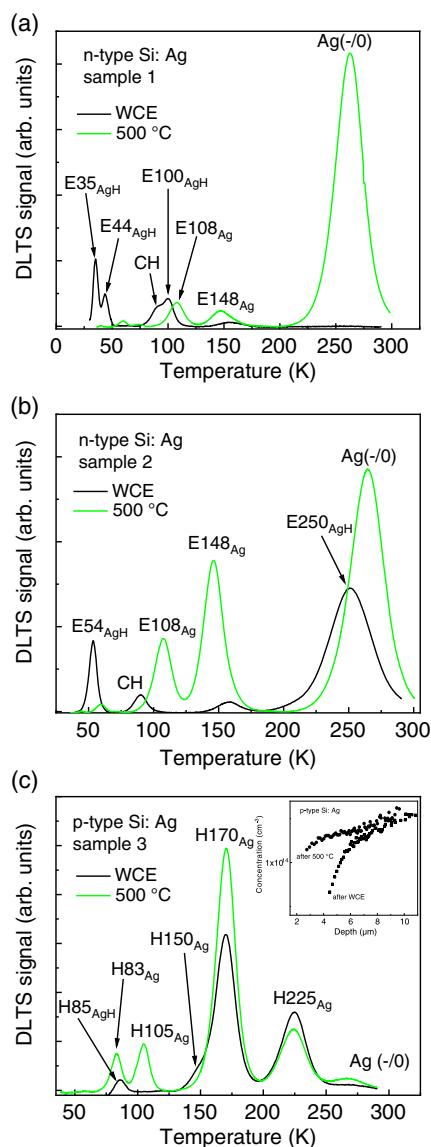


**Figure 1.** DLTS spectra recorded in samples #1 a), #2 b), and #3 c) after WCE and after annealing at 500 °C. The spectra are recorded close to the surface with a reverse bias of  $-4$  V and a filling pulse of 0 V.

$\text{Ag}^*$  observed in previous studies,<sup>[10,12]</sup> whereas  $\text{E108}_{\text{Ag}}$  has not been reported in the literature so far.

DLTS spectra in sample #2 differ significantly from those observed in sample #1.  $\text{E54}_{\text{AgH}}$  and  $\text{E250}_{\text{AgH}}$  are dominant DLTS peaks in this sample after WCE. The electrical properties of the defects corresponding to these peaks are similar to those labelled E2 and E3 in a previous study.<sup>[12]</sup> In addition to  $\text{E54}_{\text{AgH}}$  and  $\text{E250}_{\text{AgH}}$ , we also observed CH and  $\text{E158}_{\text{Ag}}$  in this sample. By measuring deeper in the bulk of the sample, Ag  $(-/0)$  becomes dominant whereas the intensity of  $\text{E54}_{\text{AgH}}$ , CH, and  $\text{E250}_{\text{AgH}}$  reduces significantly. After annealing at 500 °C three pronounced DLTS peaks  $\text{E108}_{\text{Ag}}$ ,  $\text{E148}_{\text{Ag}}$ , and Ag  $(-/0)$  were observed in sample #2 and they are similar to those observed in sample #1. In addition, a small DLTS peak can be

distinguished at around 55 K. The electrical properties of the defect corresponding to this small peak are close to those of thermal donors, which usually appear after heat treatments at such temperatures.<sup>[17]</sup>

Two DLTS peaks  $\text{H170}_{\text{Ag}}$  and  $\text{H225}_{\text{Ag}}$  were observed close to the surface in p-type Si (sample #3) after WCE and after annealing at 500 °C (Figure 1c). These peaks were also dominant when measuring deeper in the bulk of these samples. The activation enthalpy of  $\text{H170}_{\text{Ag}}$  is similar to that of Ag  $(0/+)$  reported in a previous study.<sup>[12]</sup> However, its apparent capture cross section differs by a factor of 100. In addition, several small DLTS peaks  $\text{H85}_{\text{AgH}}$  and  $\text{H150}_{\text{Ag}}$  were observed in sample #3 after WCE whereas  $\text{H83}_{\text{Ag}}$  and  $\text{H105}_{\text{Ag}}$  appeared in the annealed sample.

The inset to Figure 1c shows the distribution of the net free carrier concentration obtained from C–V measurements in sample #3 after WCE and after annealing at 500 °C. After WCE, the net free carrier concentration reduces towards the surface. We correlate this effect with the passivation of shallow acceptors by hydrogen due to the formation of electrically inactive BH complexes close to the surface. The annealing at 500 °C leads to the destruction of the BH pairs and the net free carrier concentration increases close to the surface.

Laplace DLTS measurements were used to investigate the electrical properties of the defects observed in Figure 1. Only single Laplace DLTS peaks were observed for the defects in sample #1 after WCE and after annealing at 500 °C. Figure 2 shows the Laplace DLTS spectra measured after WCE of sample #2 (Figure 2a) and sample #3 (Figure 2b,c). The spectra were recorded with two filling pulses close to the surface and deeper in the bulk at 255 K a) for sample #2 and with different reverse biases at 160 K b) and 225 K c) for sample #3. At 255 K, two distinct Laplace DLTS peaks were resolved and they were attributed to  $\text{E250}_{\text{AgH}}$  and Ag  $(-/0)$  in n-type Si (sample #2). Close to the surface the intensity of  $\text{E250}_{\text{AgH}}$  is significantly larger in comparison with that of Ag  $(-/0)$  whereas Ag  $(-/0)$  becomes dominant deeper in the bulk. We did not observe any other peaks at this temperature. The spectra recorded at 160 K in sample #3 also revealed the presence of two different Laplace DLTS peaks, labelled  $\text{H150}_{\text{Ag}}$  and  $\text{H170}_{\text{Ag}}$ , respectively. Similarly, two peaks  $\text{H210}_{\text{AgH}}$  and  $\text{H225}_{\text{Ag}}$ , which were not resolved in the conventional DLTS spectra were observed at 225 K in sample #3. By varying the reverse bias we did not observe any enhancement of the emission rates of the defects in sample #3. The activation enthalpy and the apparent capture cross sections of the defects were determined from Arrhenius plots derived from the Laplace DLTS measurements and they are combined in Table 1.

Figure 3a shows the concentration depth profiles of the defects observed in sample #2 after WCE. The concentration of PH was calculated by subtraction of the net free carrier concentration in the hydrogenated sample from the original free carrier concentration taken from the bulk. The concentrations of  $\text{E54}_{\text{AgH}}$  and  $\text{E250}_{\text{AgH}}$  are descending toward the bulk with the same slope as PH. Similarly, to the findings of Yarykin et al.,<sup>[12]</sup> a large discrepancy between these depth profiles was observed close to the surface and this difference becomes smaller in the bulk of Si. The concentration of Ag  $(-/0)$  reduces toward the surface and it reaches a constant value of around  $1.2 \times 10^{13} \text{ cm}^{-3}$  in the bulk

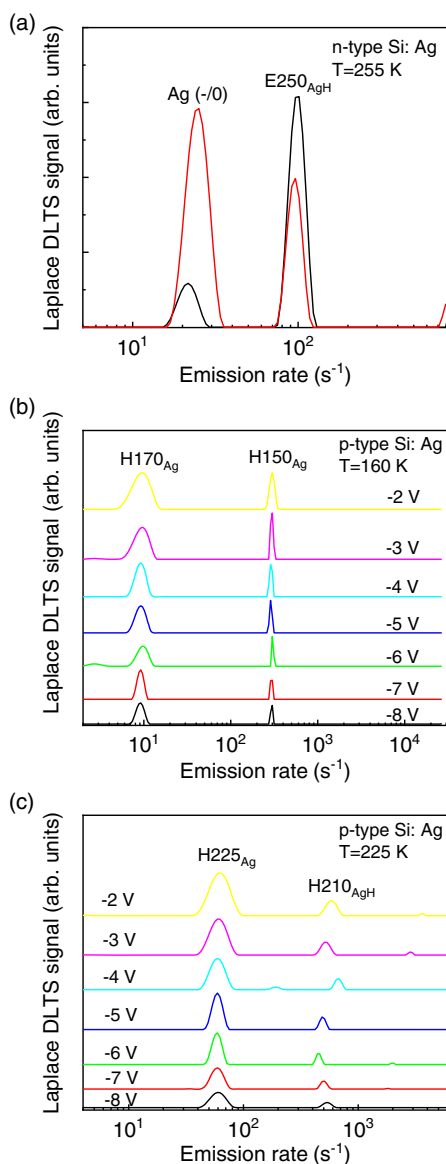


**Figure 2.** Laplace DLTS spectra recorded at 255 K in sample #2 a) and at 160 (K) b) and 225 K c) in sample #3. In sample #2, the spectra were recorded close to the surface (black line) and deeper in the bulk (red line). In sample #3, the spectra were recorded with two filling pulses (0 and  $-1$  V) by varying the reverse bias.

of Si. The concentration of Ag  $(-/0)$  in the annealed sample was almost a constant at around  $3 \times 10^{13} \text{ cm}^{-3}$ .

Figure 3b shows the depth profiles of the deep level defects observed in p-type Si (compare Figure. 1c). The concentration of BH was also obtained by subtraction of the net free carrier concentration in the hydrogenated sample from the free carrier concentration taken from the bulk of the as-grown sample. The slope of the reduction of the concentration of  $\text{H85}_{\text{AgH}}$  is similar to that of BH. The depth profile of  $\text{H225}_{\text{Ag}}$  is also decreasing toward the bulk but with a smaller slope than that of BH. In contrast, the concentration of  $\text{H150}_{\text{Ag}}$  does not vary with depth. The concentration of  $\text{H220}_{\text{AgH}}$  was too small to reliably determine

**Table 1.** Electrical properties of Ag and AgH-related defects observed in this study. The activation enthalpy and the apparent capture cross section were determined by Laplace DLTS from the Arrhenius plot ( $\ln(\text{emission rate}/T^2 \text{ vs } 1/T)$ ).

Levels	Activation enthalpy [eV]	Apparent capture cross section [ $\text{cm}^2$ ]
$\text{E35}_{\text{AgH}}$	$E_{\text{C}}-0.08$	$4 \times 10^{-13}$
$\text{E44}_{\text{AgH}}$	$E_{\text{C}}-0.09$	$2 \times 10^{-13}$
$\text{E100}_{\text{AgH}}$	$E_{\text{C}}-0.1$	$4 \times 10^{-14}$
$\text{E108}_{\text{Ag}}$	$E_{\text{C}}-0.17$	$7 \times 10^{-17}$
$\text{E148}_{\text{Ag}}$	$E_{\text{C}}-0.26$	$3 \times 10^{-16}$
$\text{E54}_{\text{AgH}}$	$E_{\text{C}}-0.09$	$1 \times 10^{-15}$
$\text{E250}_{\text{AgH}}$	$E_{\text{C}}-0.45$	$2 \times 10^{-16}$
$\text{H83}_{\text{Ag}}$	$E_{\text{V}} + 0.16$	$9 \times 10^{-15}$
$\text{H85}_{\text{AgH}}$	$E_{\text{V}} + 0.14$	$8 \times 10^{-16}$
$\text{H150}_{\text{Ag}}$	$E_{\text{V}} + 0.26$	$6 \times 10^{-16}$
$\text{H170}_{\text{Ag}}$	$E_{\text{V}} + 0.37$	$2 \times 10^{-15}$
$\text{H220}_{\text{AgH}}$	$E_{\text{V}} + 0.39$	$7 \times 10^{-14}$
$\text{H225}_{\text{Ag}}$	$E_{\text{V}} + 0.51$	$1 \times 10^{-13}$

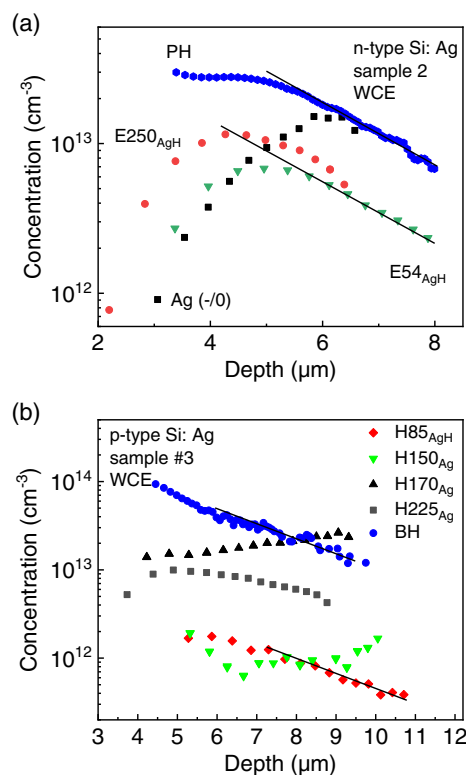


**Figure 3.** Concentration depth profiles of defects observed in samples #2 a) and #3 b) after WCE. The solid lines are fits to the defect concentrations at larger depth.

the depth profile of this defect. In samples annealed at  $500^\circ\text{C}$  the concentration of  $\text{H105}_{\text{Ag}}$ ,  $\text{H170}_{\text{Ag}}$ , and  $\text{H225}_{\text{Ag}}$  does not vary with depth. For  $\text{H170}_{\text{Ag}}$ , it is around  $2 \times 10^{13} \text{ cm}^{-3}$ .

### 3. Discussion

Different Ag-related defects were observed in n-type and p-type Si depending on the growth conditions and cooling rates of samples (compare Figure 1 and previous studies.<sup>[2,3,7,8,12]</sup>) In the as-grown sample #1 we did not observe any levels which could be correlated with Ag<sub>s</sub>, whereas it was detected in the bulk of sample #2. However, the DLTS spectra recorded in these samples after the annealing at 500 °C are similar, they exhibit three DLTS peaks E108<sub>Ag</sub>, E148<sub>Ag</sub>, and Ag (−/0). The ratio between the intensities of E108<sub>Ag</sub> or E148<sub>Ag</sub> and Ag (−/0) was significantly larger in the annealed sample #2 in comparison with that in sample #1. We explain this observation by a larger amount of Ag introduced into sample #2 during the growth. Similar to the findings of the previous studies<sup>[10,12]</sup> we assign E148<sub>Ag</sub> to the Ag–Ag pair (A\*) whereas E108<sub>Ag</sub> can be attributed to unknown Ag-related complex.

In p-type Si we also observed two dominant defects H170<sub>Ag</sub> and H225<sub>Ag</sub> which appear after the growth and two additional defects H83<sub>Ag</sub> and H105<sub>Ag</sub> detected after the annealing at 500 °C. One should also note that the intensity of H225<sub>Ag</sub> decreases in respect to H170<sub>Ag</sub> after the annealing at 500 °C. The electrical and annealing properties of H170<sub>Ag</sub> are very similar to that of Ag (0/+) reported in Yarykin et al.<sup>[12]</sup> and they might have originated from the same defect, but in this case, we cannot explain the different apparent capture cross section. We attribute H83<sub>Ag</sub>, H105<sub>Ag</sub>, and H225<sub>Ag</sub> to unknown Ag-related complexes.

Several AgH-related peaks were observed in n- and p-type Si after WCE. E35<sub>AgH</sub>, E44<sub>AgH</sub>, and E100<sub>AgH</sub> were dominant close to the surface in sample #1. None of these defects could be correlated with complexes between H and isolated substitutional Ag since we did not observe any traces of Ag (−/0) in this sample after WCE. Therefore, we tentatively attribute E35<sub>AgH</sub>, E44<sub>AgH</sub>, and E100<sub>AgH</sub> to complexes containing interstitial Ag and hydrogen. The existence of interstitial Ag was also confirmed in n- and p-type Si in Refs. [18,19] By using electron paramagnetic resonance, Son et al.<sup>[18]</sup> observed three Ag-related defects in p-type Si after the introduction of Ag at 1250 °C and subsequent quenching. The authors correlated one of the defects with an isolated interstitial silver atom whereas the two others were attributed to complexes, which contain interstitial Ag. Rollert et al.<sup>[19]</sup> investigated concentration depth profiles of Ag in dislocation free n-type Si using neutron activation analysis. The diffusivity of Ag was around  $7 \times 10^{-9} \text{ m}^2 \text{ s}^{-1}$  at 1473 K in these samples and it corresponds to the diffusion of interstitial Ag rather than Ag<sub>s</sub>.

Two DLTS levels E54<sub>AgH</sub> and E250<sub>AgH</sub> were observed close to the surface in sample #2 after WCE. As mentioned earlier, the electrical properties of the defects are similar to E3 and E2, which were previously assigned to different charge states of substitutional Ag with one H atom.<sup>[12]</sup> According to the findings of Feklisova and Yarykin,<sup>[20]</sup> the concentration of H-related defects should reduce with the same slope if they contain an identical number of H in samples after WCE. We observed that the concentration profile of E54<sub>AgH</sub> and E250<sub>AgH</sub> has the same slope as the PH and CH profiles and, therefore, we indeed attribute these defects to complexes that comprise a single H atom. However, the depth profiles of E54<sub>AgH</sub> and E250<sub>AgH</sub> as determined with high-resolution Laplace DLTS are not identical (Figure 3). This contradicts to the attribution of these defects to different

charge states of AgH<sub>2</sub>. The origin of these defects is still not clear and further studies are necessary to understand the nature of the defects or to explain the difference in their depth profiles close to the surface.

In p-type Si, we observed only one defect with a descending depth profile (H85<sub>AgH</sub>), which could be correlated with H-related defects. The concentration profile of H85<sub>AgH</sub> has the same slope as BH in p-type Si after WCE and therefore H85<sub>AgH</sub> should also contain a single H atom. This defect was not observed in the study of Yarykin et al.<sup>[12]</sup> and we tentatively correlate it with an unknown Ag–H complex. However, one could also assume that interstitial Ag is a part of this defect. The electrical properties of H210<sub>AgH</sub> are similar to those of H3,<sup>[12]</sup> but we did not find any traces of H2 in our samples although H2 and H3 were always observed together in the study of Yarykin et al.<sup>[12]</sup>

### 4. Conclusion

In the present study, we reinvestigated the electrical properties of Ag- and AgH-related defects in n- and p-type Si by DLTS and Laplace DLTS measurements. Different defects were observed in these samples depending on their growth conditions and heat treatments. Several AgH-related peaks, which were not previously reported in the literature were also observed in hydrogenated n- and p-type Si. We investigated their depth profiles and discussed their origin. By using Laplace DLTS measurements, we questioned the origin of the peaks (E6, E2, and E3) previously attributed to Ag<sub>s</sub>H and Ag<sub>s</sub>H<sub>2</sub> in Yarykin et al.<sup>[12]</sup>

### 5. Experimental Section

N-type and p-type float-zone Si samples with a doping concentration of  $2 \times 10^{14} \text{ cm}^{-3}$  of P or B were used. Silver was incorporated during the crystal growth ( $[\text{Au}_s] < 1 \times 10^{14} \text{ cm}^{-3}$ ). Samples were cut from crystals grown with different concentrations of Ag (15 mg into sample #1 and 30 mg into samples #2 and #3). The as-grown samples were polished by wet chemical etching (WCE) in CP4A (HF:HNO<sub>3</sub>:CH<sub>3</sub>COOH 3:5:3) at room temperature for 10 min. Several samples were annealed at 500 °C in air. Schottky-contacts were fabricated by resistive evaporation of Au (n-type) or Al (p-type) through a shadow mask. Ohmic contacts were made by rubbing a eutectic InGa-alloy into the backside of the samples. The quality of the Schottky and Ohmic contacts was checked by current-voltage and capacitance-voltage (C–V) measurements at room temperature and at 50 K. The C–V curves were recorded at 1 MHz. Conventional DLTS and Laplace DLTS were used to investigate the properties of the defects. The concentration depth profiles were obtained using the double pulse Laplace DLTS technique as described in the previous study.<sup>[15]</sup> For the calculation of the concentration the temperature dependent  $\lambda$ -layer was taken into account.<sup>[21]</sup> The electric field was calculated from the C–V measurements as described in Ref. [21]. The levels are labelled using E or H (for electron or hole traps, respectively) followed by the temperature at which the peaks appear in the DLTS spectrum for an emission rate of  $50 \text{ s}^{-1}$ .

### Acknowledgements

The authors thank Leibniz-Institut für Kristallzüchtung (IKZ), Berlin, for supplying the samples, and R. Stübner for useful discussions. K.G. thanks the German Academic Exchange Service (DAAD) for the support of her stay in Dresden and also acknowledges Wrocław University of Science and Technology statutory grant (no. 8211104160).

Open access funding enabled and organized by Projekt DEAL.

## Conflict of Interest

The authors declare no conflict of interest.

## Data Availability Statement

Research data are not shared.

## Keywords

defects, deep-level transient spectroscopy (DLTS), Laplace DLTS, silicon, silver

Received: April 15, 2021  
Revised: July 2, 2021  
Published online: July 29, 2021

- 
- [1] H. Irmeler, Z. Naturforsch, **1958**, 13a, 557.
  - [2] L. D. Yau, C. T. Sah, *Phys. Stat. Sol. A* **1971**, 6, 561.
  - [3] L. D. Yau, C. F. Smiley, C. T. Sah, *Phys. Stat. Sol. A* **1972**, 13, 457.
  - [4] F. L. Thiel, S. K. Gandhi, *J. Appl. Phys.* **1970**, 41, 254.
  - [5] W. Fahrner, A. Goetzberger, *Appl. Phys. Lett.* **1972**, 21, 329.
  - [6] A. J. Tavendale, S. J. Pearton, *J. Phys. C* **1983**, 16, 1665.
  - [7] N. Baber, H. G. Grimmeiss, M. Kleverman, P. Omling, M. Zafar Iqbal, *J. Appl. Phys.* **1987**, 62, 2853.
  - [8] H. Lemke, *Phys. Stat. Sol. A* **1986**, 94, K55.
  - [9] S. J. Pearton, A. J. Tavendale, *J. Phys. C* **1984**, 17, 6701.
  - [10] H. Lemke, *Mater. Sci. Forum* **1995**, 196, 683.
  - [11] J. Olajos, M. Kleverman, G. Grimmeiss, *Phys. Rev. B* **1988**, 38, 633.
  - [12] N. Yarykin, J.-U. Sachse, H. Lemke, J. Weber, *Phys. Rev. B* **1999**, 59, 5551.
  - [13] G. Davies, T. Gregorkiewicz, M. Zafar Iqbal, M. Kleverman, E. C. Lightowers, N. Q. Vinh, M. Zhu, *Phys. Rev. B* **2003**, 67, 235111.
  - [14] A. Resende, R. Jones, S. Öberg, P. R. Briddon, *Phys. Rev. Lett.* **1998**, 82, 2111.
  - [15] L. Dobaczewski, A. R. Peaker, K. Bonde Nielsen, *J. Appl. Phys.* **2004**, 96, 4689.
  - [16] R. Stübner, *J. Appl. Phys.* **2015**, 118, 055704.
  - [17] K. Gwozdz, *Phys. Stat. Sol. A* **2019**, 216, 1900302.
  - [18] N. T. Son, V. E. Kustov, T. Gregorkiewicz, C. A. J. Ammerlaan, *Phys. Rev. B* **1992**, 46, 4544.
  - [19] F. Rollert, N. A. Stolwijk, H. Mehrer, *J. Phys. D: Appl. Phys.* **1987**, 20, 1148.
  - [20] O. Feklisova, N. Yarykin, *Semicond. Sci. Technol.* **1997**, 12, 742.
  - [21] P. Blood, P. W. Orton, in *The Electrical Characterization of Semiconductors: Majority Carriers and Electron States* (Ed: N.H. March), Academic Press, Cambridge, MA **1992**, pp. 661–674.